Supplementary Material for "A Second Order Cone Programming Model for PEV Fast-Charging Station Planning"

Hongcai Zhang, *Student Member, IEEE,* Scott J. Moura, *Member, IEEE,* Zechun Hu, *Member, IEEE,* Wei Qi, and Yonghua Song, *Fellow, IEEE*

Abstract

In this supplementary material, we first describe the detailed information of the test system in the paper "A Second Order Cone Programming Model for PEV Fast-Charging Station Planning". Note that these parameter values are for illustration and not necessarily representative of a particular transportation/power system network. Readers are encouraged to substitute their own parameter values. Then, we provide the details of the scenarios of base load profiles, traffic flow curves etc. that we utilize in the case studies. At last, we conduct some supplementary experiments to validate the influence of power network constraints on the planning results and the performance of the proposed service rate model.

I. Parameters of the Distribution System

The diagram of the 110 kV high voltage distribution network is shown in Fig. 1. We assume node 1 is connected to a 220 kV/110 kV transformer with 150 MVA capacity.

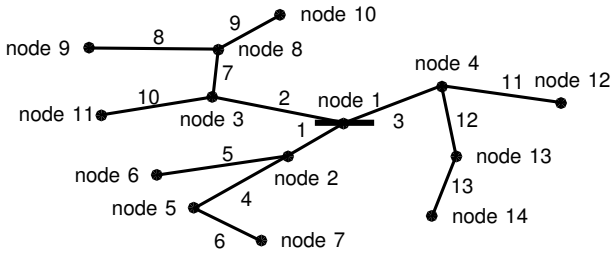

Fig. 1. A 110 kV distribution network used for the case study.

A. Branch Parameters

The branch parameters are listed in Table I.

B. Load Data

The peak load data are listed in Table II. The load at each node is assumed to be composed by residential load, commercial load and agricultural load.

II. Scenario Preparation for the Case Studies

A. Load Profile Scenario

We used PG&E static residential, commercial and agricultural load profiles [1] to generate 24 representative scenarios, i.e., weekday and weekend of 12 months, of three types of load profiles, which are respectively shown in Figs. 2–4. Then the time-varying load at each bus i is calculated as follows:

$$L_i(\omega,t) = \overline{L_i} \times \left(\alpha_i^{\mathrm{R}} \times L^{\mathrm{R}}(\omega,t) + \alpha_i^{\mathrm{C}} \times L^{\mathrm{C}}(\omega,t) + \alpha_i^{\mathrm{A}} \times L^{\mathrm{A}}(\omega,t)\right). \tag{1}$$

Where, $\overline{L_i}$ is the summation of active load, reactive load and compensation given in Table I, which is the peak load in a day. α_i^{R}, α_i^{C} and α_i^{A} are representatively the load component ratio of residential, commercial and agricultural load given in Table I. $L^{\mathrm{R}}(\omega,t)$, $L^{\mathrm{C}}(\omega,t)$, $L^{\mathrm{A}}(\omega,t)$ are respectively the corresponding per-unit load profiles of each scenario.

H. Zhang, Z. Hu and Y. Song are with the Department of Electrical Engineering, Tsinghua University, Beijing, 100084, P. R. China (email: zechhu@tsinghua.edu.cn).

S. J. Moura is with the Department of Civil and Environmental Engineering, University of California, Berkeley, California, 94720, USA.

W. Qi is with the Department of Industrial Engineering and Operations Research, University of California, Berkeley, California, 94720, USA.

TABLE I
BRANCH PARAMETERS OF THE DISTRIBUTION NETWORK

Branch ID	From Bus	To Bus	Length(km)	R (p.u.)	X (p.u.)	Capacity (MVA)
1	1	2	30	0.0317	0.0760	50.00
2	1	3	70	0.0739	0.1774	50.00
3	1	4	20	0.0211	0.0507	50.00
4	2	5	110	0.1793	0.2870	27.00
5	2	6	70	0.1952	0.1913	20.25
6	5	7	60	0.1674	0.1640	20.25
7	3	8	50	0.0815	0.1305	27.00
8	8	9	30	0.0837	0.0820	20.25
9	8	10	40	0.1116	0.1093	20.25
10	3	11	60	0.1674	0.1640	20.25
11	4	12	40	0.1116	0.1093	20.25
12	4	13	80	0.1304	0.2088	27.00
13	13	14	60	0.1674	0.1640	20.25

TABLE II
LOAD DATA OF THE DISTRIBUTION NETWORK

Bus ID	Active load (MW)	Reactive load (MVAR)	Reactive compensation (MVAR)	Load Component (%)		
				Residential	Commercial	Agricultural
1	0	0	0	0	0	0
2	3.7500	3.0000	0	40	50	10
3	7.5000	5.0625	0	40	50	10
4	1.8750	1.6875	0	40	50	10
5	3.7500	1.5000	0.4688	40	40	20
6	5.6250	2.8125	0.3750	40	40	20
7	2.8125	2.2500	0	40	30	30
8	9.3750	5.6250	2.2500	40	30	30
9	8.4375	3.7500	9.3750	40	20	40
10	1.1250	0.1875	1.1250	40	20	40
11	1.8750	1.6875	3.3750	40	20	40
12	1.8750	1.3125	0	40	10	50
13	1.8750	1.6875	0	40	10	50
14	3.9375	1.8750	3.3750	40	10	50

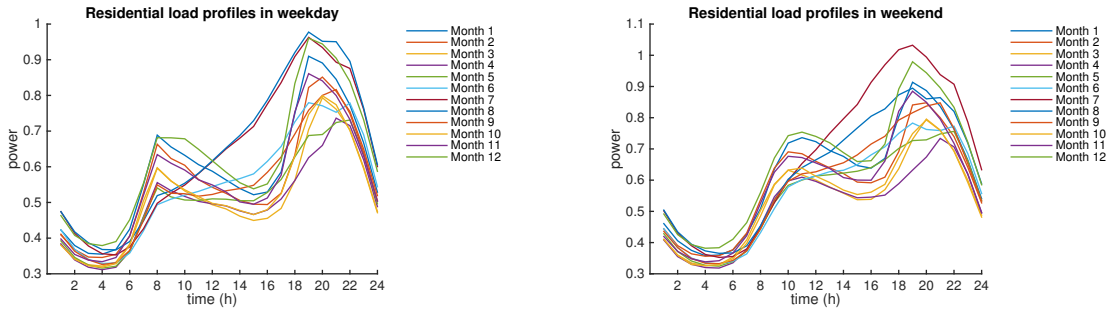

Fig. 2. Residential load profiles.

B. Traffic Flow Scenario

The traffic flow scenarios are generated from NHTS data [2]. First, we generate the distribution of departure time from home every day, i.e., D, in [2] (note that only the first departure event is used). Then, we assume the PEVs arrive at the transportation network according to the distribution D and travel in the transportation network with an average speed of 80 km/h. Thereafter, we calculate the traffic flow arriving at each transportation node based on the distribution D of time when PEVs arrive at the transportation network, driving speed and driving paths.

Take a single path as an example. Let 0 denote the arrival node, then the traffic flow node 0, i.e., $\lambda_0(t)$, follows the distribution D. Then the traffic flow of node i on the same path can be calculated as:

$$\lambda_i(t + \frac{d_{i0}}{v}) = \lambda_0(t), \tag{2}$$

where, d_{i0} is the distance between node 0 and node i; $v = 80$km/h is the expected drive speed.

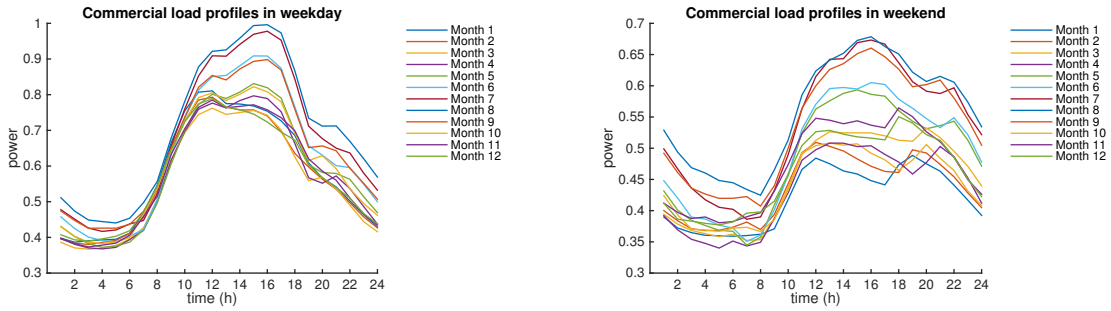

Fig. 3. Commercial load profiles.

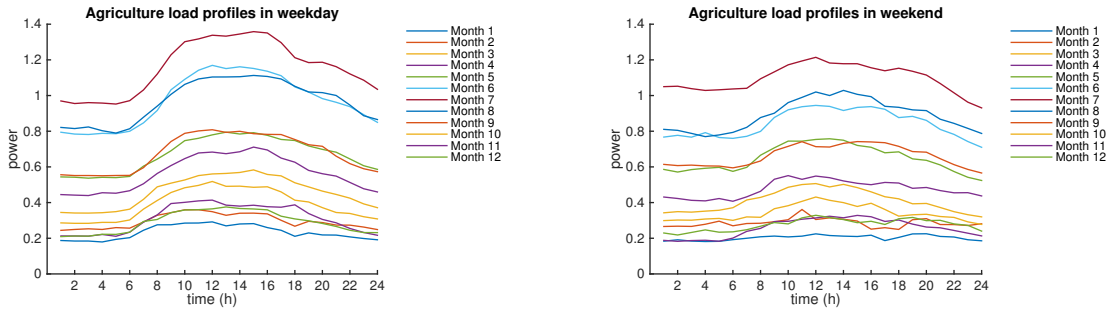

Fig. 4. Agricultural load profiles.

Because NHTS data does not distinguish weekday and weekend, therefore, we simply assume the original distribution D is the distribution in weekday and we generate the distribution in weekend by decreasing the total traffic flow by 20%. We also assume all the arrival distributions D in all the12 month are the same.

The distributions of the time when PEVs arrive at the transportation network in weekday and weekend are illustrated in Fig. 5. Note that these traffic flow profiles are for illustrative purpose only. In practice, we can easily adopt actual traffic flow data in our planning model.

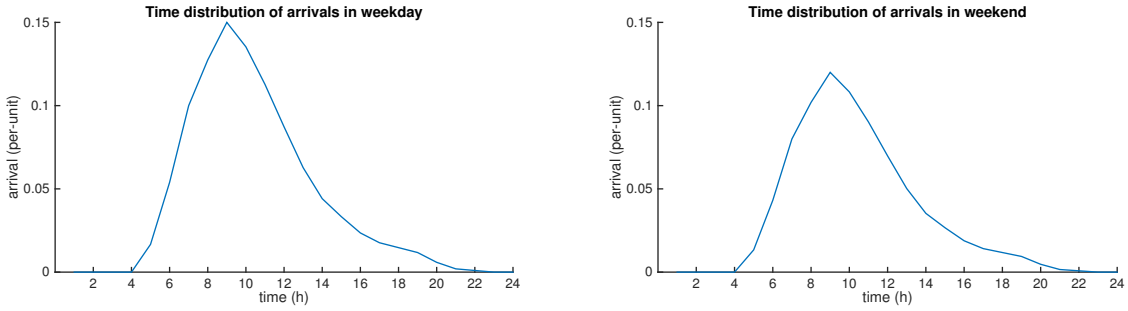

Fig. 5. Distributions of the time when PEVs arrive at the transportation network.

III. Supplementary Experiments

This section provides supplementary experiments for the main body.

A. The Influence of Power Network Constraints

We designed two extra cases, i.e., Cases 5-6, in addition to the four cases in the paper to demonstrate the benefits when jointly considering transportation and power network constraints. The parameters of Cases 5 and 6 are respectively the same with those of Cases 1 and 4, except that the power network constraints and the distribution system upgrade costs in Cases 5 and 6 are ignored. The parameters of Cases 1, 4-6 are demonstrated in Table III.

The summary of the planning results are illustrated in Table IV.

When ignoring the power network constraints, i.e., the AC power flow constraints, the unsatisfied PEV charging demands will increase. In Case 1, all the PEV charging demands are satisfied; while, in Case 5, 0.034% of the PEV charging demands

TABLE III
SUPPLEMENTARY BENCHMARK CASES OF THE PLANNING

Case	Distribution system upgrade costs	Power network constraints	Traffic flow per day (of the highest traffic scenario)
1	Consider	Consider	20000
4	Consider	Consider	40000
5	Ignore	Ignore	20000
6	Ignore	Ignore	40000

TABLE IV
THE PLANNING RESULTS OF DIFFERENT CASES

Case	Station no.	Spot no.	Expected annual costs (M$)				Unsatisfied PEV load (%)	Binary variable no.	Solution time (min)
			Station Investment	Grid upgrade	Electricity	Total			
1	28	1169	5.13	4.37	38.33	47.83	0	5,761	9.37
4	45	2340	9.91	12.41	49.27	71.59	1.89	5,761	11.10
5	21	1160	4.88	6.47	38.45	49.80	0.034	5,761	16.81
6	26	2211	8.99	12.64	48.27	69.89	4.53	5,761	30.67

can not be fulfilled. Compared with Case 4, the ratio of unsatisfied PEV charging demands of Case 6 increased significantly by 139.7%. When the PEV population is large and the power supply capacities are binding in some distribution nodes, the planner prefers to invest more charging stations elsewhere to avoid distribution system thermal congestion. As a result, the numbers of charging stations and spots in Case 4 are much higher than those in Case 6.

When ignoring the distribution system upgrade costs in the planning model, the planner may conduct myopic investment decisions based on limited information. As a result, though the PEV charging station investment costs may be minimized, the system planner has to invest more in distribution system upgrades, which will surpass the savings in PEV charging station investments. This is predominant under low PEV population scenarios when almost all the PEV charging demands can be satisfied. Considering distribution system upgrade costs helps to reduce total investment costs.

B. Performance of the Service Rate Model

This section conducts experiments to validate the performance of the proposed service rate model.

We utilize the proposed model to design the capacities of charging stations under different PEV Poisson arrival parameters, i.e., from 20 to 300 PEVs/h, and different service rate levels, i.e., from 70% to 90%. We also assume four types of PEVs on road with equal market share, and their driving ranges per charge are respectively 200, 300, 400 and 500 km . The average service time to recharge the four different types of PEVs with empty batteries is about 42, 63, 84, 105 minutes.

Then, we utilize the Monte-Carlo method [3] to simulate the real-time operations including PEV arriving, charging and leaving behaviors of the designed charging stations for 5000 hours.

1) Accuracy of the Service Rate Model: We first assume that the charging stations are operated based on the *first-in-first-out* rule in assumption [A2]. We counted the number of unsatisfied charging demands (those leave before getting charged for their required time units), the corresponding actual service rates are listed in Fig. 6.

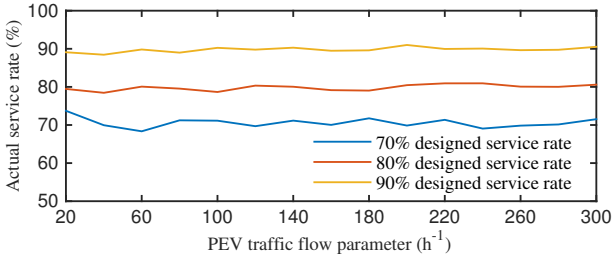

Fig. 6. Accuracy of the service rate model.

We can see that the actual service rates in the experiments are very close to the designed values under different PEV Poisson arrival parameters and designed service rate levels. This proves that the proposed service rate model is accurate.

2) Waiting Time Analysis in Real-time Operations: We then assume that the PEVs will wait in the station if all the charging spots are occupied until one PEV has got fully charged and spare a spot for it. We calculated two service quality criterions, i.e., the ratios that the PEVs get instantly charged without waiting (see Fig. 7), and the average waiting time of all the PEVs (see Fig. 8).

On one hand, the experiment results show that the probabilities that the PEVs get instantly charged without waiting are close to the designed service rate levels. This is especially true when the designed service rate level is high and few PEVs have to wait. On the other hand, even though the two values, i.e., the probability of instant service and the designed service rate, are not equal; the former is still well controlled by the latter. The results show that the differences between the two values under different designed service rate levels are stable and insensitive to the volumes of the PEV arrivals. That means, we can realize an one-to-one mapping between the two values so that we can use the service rate to accurately control the probability of instant charging service (or probability of waiting).

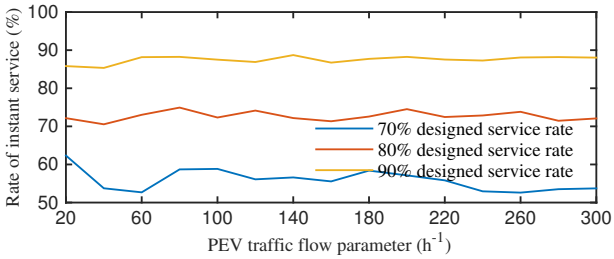

Fig. 7. Probabilities that the PEVs get instant charging services.

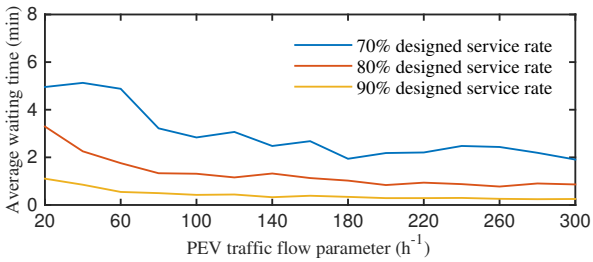

Fig. 8. Average waiting time.

We can also conclude from Fig. 8 that the average waiting time of the PEVs are also well controlled by the designed service rate level. When the service rate level increases, the average waiting time decreases.

Therefore, though the assumption [A2] may be not true in practice, the service rate in the proposed model is still meaningful because it provides the system planner an intuitive and specific service quality criterion for the designed system.

REFERENCES

[1] PG&E, "2000 static load profiles." [Online]. Available: https://www.pge.com/nots/rates/2000_static.shtml, accessed Sep 30, 2016.
[2] A. Santos, N. McGuckin, H. Y. Nakamoto, D. Gray, and S. Liss, "Summary of travel trends: 2009 national household travel survey," tech. rep., 2011.
[3] C. Z. Mooney, *Monte carlo simulation*, vol. 116. Sage Publications, 1997.